

# UC Davis

## UC Davis Previously Published Works

### Title

Overlapping Local and Systemic Defense Induced by an Oomycete Fatty Acid MAMP and Brown Seaweed Extract in Tomato

### Permalink

<https://escholarship.org/uc/item/6b27j313>

### Journal

Molecular Plant-Microbe Interactions, 36(6)

### ISSN

0894-0282

### Authors

Lewis, Domonique C  
Stevens, Danielle M  
Little, Holly  
[et al.](#)

### Publication Date

2023-06-01

### DOI

10.1094/mpmi-09-22-0192-r

Peer reviewed



Published in final edited form as:

*Mol Plant Microbe Interact.* 2023 June ; 36(6): 359–371. doi:10.1094/MPMI-09-22-0192-R.

## Overlapping Local and Systemic Defense Induced by an Oomycete Fatty Acid MAMP and Brown Seaweed Extract in Tomato

Domonique C. Lewis<sup>1</sup>, Danielle M. Stevens<sup>1</sup>, Holly Little<sup>2</sup>, Gitta L. Coaker<sup>1</sup>, Richard M. Bostock<sup>1,†</sup>

<sup>1</sup>Department of Plant Pathology, University of California, Davis, CA 95616, U.S.A.

<sup>2</sup>Acadian Plant Health, Acadian Seaplants Limited, Dartmouth, Nova Scotia, Canada

### Abstract

Eicosapolyenoic fatty acids are integral components of oomycete pathogens that can act as microbe-associated molecular patterns to induce disease resistance in plants. Defense-inducing eicosapolyenoic fatty acids include arachidonic acid (AA) and eicosapentaenoic acid and are strong elicitors in solanaceous plants, with bioactivity in other plant families. Similarly, extracts of a brown seaweed, *Ascophyllum nodosum*, used in sustainable agriculture as a biostimulant of plant growth, may also induce disease resistance. *A. nodosum*, similar to other macroalgae, is rich in eicosapolyenoic fatty acids, which comprise as much as 25% of total fatty acid composition. We investigated the response of roots and leaves from AA or a commercial *A. nodosum* extract (ANE) on root-treated tomatoes via RNA sequencing, phytohormone profiling, and disease assays. AA and ANE significantly altered transcriptional profiles relative to control plants, inducing numerous defense-related genes with both substantial overlap and differences in gene expression patterns. Root treatment with AA and, to a lesser extent, ANE also altered both salicylic acid and jasmonic acid levels while inducing local and systemic resistance to oomycete and bacterial pathogen challenge. Thus, our study highlights overlap in both local and systemic defense induced by AA and ANE, with potential for inducing broad-spectrum resistance against pathogens.

### Keywords

arachidonic acid; *Ascophyllum nodosum*; *Phytophthora capsici*; plant immunity; *Pseudomonas syringae* pv. *tomato*; *Solanum lycopersicum*

---

Members of Phaeophyta and Rhodophyta—brown and red macroalgae—contain multiple bioactive molecules and derived oligosaccharides that are known to induce defense responses in plants (Klarzynski et al. 2003; Sangha et al. 2010; Vera et al. 2011).

*Ascophyllum nodosum*, a brown alga (seaweed), is a rich source of polyunsaturated fatty

---

This is an open access article distributed under the [CC BY-NC-ND 4.0 International license](https://creativecommons.org/licenses/by-nc-nd/4.0/).

<sup>†</sup>Corresponding author: R. M. Bostock; rmbostock@ucdavis.edu.

e-Xtra: Supplementary material is available online.

The author(s) declare no conflict of interest.

acids, including the eicosapolyenoic acids arachidonic acid (AA) and eicosapentaenoic acid (EPA), which comprise as much as 25% of total fatty acid composition (Lorenzo et al. 2017; van Ginneken et al. 2011). AA and EPA are essential fatty acids found in lipids and cell walls of oomycete pathogens, are absent from higher plants, and have specific structural requirements for elicitor activity (Araceli et al. 2007; Creamer and Bostock 1986; Gellerman et al. 1975). Algal species like *A. nodosum* belong to the same major eukaryotic lineage as oomycetes, the Stramenopila. AA and EPA are potent oomycete-derived elicitors of plant defenses, and their elicitor activity is strongly enhanced by branched  $\beta$ -glucan oligosaccharins (Bostock et al. 1981; Robinson and Bostock 2015). AA, EPA, and other eicosapolyenoic acids can be considered microbe-associated molecular patterns (MAMPs), although their initial perception and signaling is likely different than canonical MAMPs directly perceived by cell-surface receptors (Ngou et al. 2022). Eicosapolyenoic acids are released by *Phytophthora infestans* spores and hyphae during infection of potato leaves and are taken up and incorporated into host plant cell lipids or oxidized to hydroperoxy acids and uncharacterized products (Fournier et al. 1993; Göbel et al. 2001, 2002; Hwang and Hwang 2010; Preisig and Ku 1988; Ricker and Bostock 1992; Véronési et al. 1996). Representing a novel class of MAMPs, AA and EPA engage hormone-mediated immune pathways in plants (Fidantsef and Bostock 1998; Savchenko et al. 2010).

Extracts from *A. nodosum* are used in agriculture primarily to stimulate plant growth and development but may also increase biotic and abiotic stress tolerances (Shukla et al. 2019). There are various commercial formulations of *A. nodosum* extracts, and each is a unique proprietary mixture. When compared, these products elicit varying transcriptional outcomes in plants (Goñi et al. 2016). The commercial *A. nodosum* extract Acadian (hereafter, ANE) (Acadian Seaplants, Ltd., Dartmouth, Canada), is a biostimulant that can also protect plants against fungal and bacterial pathogens (Ali et al. 2016; Jayaraj et al. 2008). In *Arabidopsis thaliana*, ANE induces systemic resistance to *Pseudomonas syringae* pv. *tomato* and *Sclerotinia sclerotiorum* (Subramanian et al. 2011). Studies on ANE-induced disease resistance in *Arabidopsis thaliana* and tomato implicate jasmonic acid (JA)-dependent signaling, increased reactive oxygen species (ROS) production, induction of numerous immune response genes, and increased defense-related proteins and metabolites (Ali et al. 2016; Cook et al. 2018; Jayaraj et al. 2008; Subramanian et al. 2011). As the predominant polyunsaturated fatty acid in *A. nodosum*, AA may contribute to ANE biological activity. The ability of these eicosapolyenoic acids to induce resistance to diverse pathogens and trigger phytoalexin accumulation, lignin, ROS, and programmed cell death has been shown in solanaceous and other plant families (Araceli et al. 2007; Bostock et al. 1981; Cook et al. 2018; Dye et al. 2020; Knight et al. 2001).

Here, we investigate the overlap in plant response to AA and ANE. In this study, 3' batch tag sequencing (Lohman et al. 2016; Meyer et al. 2011) was used to compare and contrast AA- and ANE-induced transcriptomes locally in treated roots and systemically in leaves of root-treated tomato seedlings, revealing extensive overlap. Using disease assays with seedlings challenged with *Phytophthora capsici* and the bacterial speck pathogen *Pseudomonas syringae* pv. *tomato*, we demonstrate the systemicity of AA- and ANE-induced resistance in tomato. The effect of AA and ANE root treatments on levels of selected phytohormones in roots and leaves also were determined to establish the

relationship between transcriptional reprogramming and phytohormone changes that may prime or influence host defense.

## Results

### Transcriptomic analyses of AA- and ANE-induced plants.

We hypothesized that AA- and ANE-induced resistance may be mediated by similar or shared transcriptional changes locally, in treated roots, and systemically, in leaves of root-treated tomato seedlings. To investigate transcriptomes of AA- and ANE-treated tomato (*Solanum lycopersicum* cv. New Yorker), roots of hydroponically grown seedlings were treated with 10  $\mu$ M AA, 0.4% ANE, 10  $\mu$ M linoleic acid (LA), or H<sub>2</sub>O for 6, 24, and 48 h prior to harvesting and processing for RNA sequencing (Fig. 1A). Water and LA, an abundant fatty acid in plants, were included as negative controls. Of the sequencing reads across all samples, 65.3 to 85.7% uniquely mapped to the tomato reference genome build SL 3.0 (Supplementary Fig. S1). Principal component analysis (PCA) of normalized read count data revealed distinct clustering of treatment groups across all tested timepoints in root tissue (Fig. 1B, C, and D). Both AA and ANE treatments exhibited unique clusters, whereas control treatments H<sub>2</sub>O and LA clustered together at 6, 24, and 48 h in roots. PCAs of read count data for leaf tissue showed similar but less distinct clustering across treatments and timepoints, reflective of distal tissue (Supplementary Fig. S2). The most distinct clustering in leaves was observed at 24 h, when both negative controls, H<sub>2</sub>O and LA, overlapped. Partial overlap between AA and ANE treatment groups was also observed at 24 h in leaf tissue. Similarly, heatmaps visualizing normalized read counts of the most differentially expressed genes (DEGs) by fold change at 24 h showed distinct clustering by treatment group in both roots (Fig. 2A) and leaves (Fig. 2B). DEGs were set at an absolute fold change cutoff  $>4$  for roots and  $>2$  for leaves, with adjusted *P* values  $<0.05$  across all timepoints and treatments. Heatmaps of transcriptomes depict clear grouping of profiles across both sampled tissues. Gene expression profiles of H<sub>2</sub>O and LA treatments were nearly indistinguishable but clearly distinct from the profiles resulting from AA and ANE treatments (Figs. 1 and 2). AA and ANE induced robust transcriptional changes relative to control treatments (Figs. 1 and 2), with both elicitors effecting significant overlap in gene expression profiles as well as notable differences between treatments.

Root treatment with AA and ANE induced transcriptional changes relative to the H<sub>2</sub>O control both locally (roots) and systemically (leaves) with varying temporal dynamics. In AA-treated plants, transcriptional reprogramming occurred most strongly at 24 h in roots and leaves (Fig. 3A). ANE-treated plants showed transcriptional changes most strongly at 6 h in roots and 24 h in leaves (Fig. 3A; Supplementary Fig. S3). Roots and leaves of either AA or ANE root-treated tomato seedlings have many shared DEGs, with AA-treated plants exhibiting the most numerous changes in gene expression. Within a tissue, roots and leaves shared up- and downregulated DEGs for both AA and ANE treatments, with roots showing more DEGs than leaves (609 induced and 382 suppressed genes at 24 h) (Fig. 3C). By comparison, leaves had 85 induced and 104 suppressed genes at 24 h (Supplementary Fig. S3).

Although AA and ANE root treatments altered expression of many of the same genes, these treatments also induced distinct transcriptome features in roots and leaves. Of genes that were unique to each treatment, roots displayed a higher number of these features, with 1,671 genes identified in roots compared with 362 genes in leaves (Fig. 3C). At the earliest tested timepoint, the transcriptional profile of ANE-treated roots revealed more than 76% unique DEGs. At 24- and 48-h timepoints, AA- and ANE-treated roots showed the most overlap in transcriptional changes, with some 992 and 728 shared DEGs, respectively. Analysis of distal untreated leaf tissue also revealed a similar trend, with overlap in shared DEGs occurring most robustly at 24 and 48 h (Supplementary Fig. S3D). Distinct transcriptional features in the leaves of AA and ANE root-treated plants can be seen across all tested timepoints, with more than 61 and 45% of identified DEGs being specific to their respective treatment group at 24 h (Supplementary Fig. S3).

### **Treatment with AA and ANE induces upregulation of transcripts involved in oxylipins, immunity, and secondary metabolism.**

In order to identify specific gene categories and biological processes altered by AA and ANE treatments, we performed gene ontology (GO) functional analyses. GO analyses revealed AA and ANE root treatments enrich similar categories of tomato genes in both molecular function and biological processes categories (Fig. 4A and B). AA- and ANE-enriched root transcripts associated with oxidation-reduction processes, including hydrogen peroxide catabolism, oxidative-stress responses, and heme binding. Both treatments induced cell-wall macromolecule catabolism genes as well as a variety of genes classically associated with defense responses.

Identification of specific defense- and stress-related genes significantly induced in AA- and ANE-treated roots at 24 h revealed insightful overlap (Fig. 5). Transcripts of several key genes in biosynthesis of plant oxylipins, including *α-DOXI*, *9-DES*, *9-LOX*, and *AOS3*, were significantly up-regulated in response to AA and ANE root treatment. This corresponds with early work that first implicated oxylipin metabolism in AA action and demonstrated the capacity of plant endogenous *9-LOX* to use AA as a substrate (Andreou et al. 2009; Fournier et al. 1993; Göbel et al. 2001, 2002; Hwang and Hwang 2010; Véronési et al. 1996). The phytohormone JA and related metabolites are also oxylipins (Dave and Graham 2012). We observed induction of multiple JA-responsive genes including *JA2*, *JA2L*, *SIJAZ7*, and *SIJAZ11* (Sun et al. 2011), which previous studies reported were induced in response to *Pseudomonas syringae* pv. *tomato* infection or exogenous application of various phytohormones (Chini et al. 2017; Du et al. 2014; Ishiga et al. 2013).

AA and ANE similarly induced genes encoding known immune signaling components in roots at 24 h. Significant increase in expression was seen in genes encoding mitogen-activated protein kinase kinase kinases and several WRKY transcription factors, including *SIWRKY39*, which confers enhanced resistance to biotic and abiotic stressors upon overexpression in transgenic tomato (Sun et al. 2015). Accumulation of salicylic acid (SA) and induction of SA-responsive genes are hallmarks of plant immune responses, including MAMP perception (Chen et al. 2017; Tsuda et al. 2009). In roots at 24 h, we observed upregulation of *NPR1* (Fig. 5), encoding a SA receptor that positively regulates expression

of SA-dependent genes and is considered a master regulator of SA signaling (Chen et al. 2017). Likewise, the SA marker and pathogenesis-related (PR) gene *PR-1* showed induction in roots at 24 h. Shared concurrent induction of these immunity-related genes indicate plants exposed to AA and ANE are generally primed for defense against a wide array of potential pathogen challenge.

Genes involved in secondary metabolism also showed strong induction in roots at 24 h. Shikimate pathway members *PAL* (phenylalanine ammonia lyase) and *CS1* (chorismate synthase) had increased expression compared with water in AA- and ANE-treated roots. Upregulation of genes involved in metabolism of other phenolic compounds included *THT1-3* (tyramine n-hydroxycinnamoyl transferase) and a polyphenol oxidase. The sesquiterpenoid biosynthesis gene TSP31 (viridiflorene synthase) showed significant induction with an increase in  $\log_2$  fold change of 9.29 and 5.66 for AA and ANE, respectively, compared with water. Genes for key early steps in terpenoid biosynthesis, 3-hydroxy-3-methylglutaryl coenzyme A synthase (*HMGCS*) and 3-hydroxy-3-methylglutaryl coenzyme A reductase 2 (*HMGCR2*), a pathogen- and elicitor-responsive isoform, showed robust increases in expression in both treatment groups (Choi et al. 1992; Stermer and Bostock 1987).

To assess global trends in transcriptional remodeling, GO functional analyses of AA- and ANE-treated tomato revealed significant congruency in under-represented gene categories. Nearly perfect overlap was seen in all unenriched GO terms in molecular function, biological process, and cellular compartment in roots at 24 h (Supplementary Table S1). Examination of specific shared genes most strongly downregulated in response to AA and ANE treatment revealed suppression of genes associated with metal transport (Supplementary Table S2). This included genes annotated to operate as metal, iron-regulated and copper transporters, and metal tolerance in roots at 24 h. The uptake and translocation of nutrient metals is essential for plant growth and development (Jogawat et al. 2021). The downregulation of these transporters may indicate a shift toward defense rather than growth in the plant.

### **Transcriptional changes specific to AA and to ANE treatments.**

Considering the difference in composition of AA and ANE, we examined the strongest uniquely up- and downregulated genes in roots at 24 h (Supplementary Table S3). Unique transcriptional responses for AA-treated plants revealed differential expression of ethylene and terpene biosynthesis genes and modulation of genes involved in auxin signaling, cell-wall anabolism, and signaling peptide formation. This included significant induction of *ACS2* (1-aminocyclopropane-1-carboxylate synthase 2), encoding an isoform that catalyzes the synthesis of the ethylene precursor 1-aminocyclopropane carboxylic acid, and suppression of an *ACO* isoform encoding 1-aminocyclopropane-1-carboxylate oxidase-like protein, the terminal step in ethylene synthesis. This suggests a degree of fine regulation of ethylene production in roots in response to AA. Unique upregulation was also seen in a purported sesquiterpene synthase gene that showed a  $\log_2$  fold change of 5.02 compared with H<sub>2</sub>O. Unique differential gene expression after AA treatment was also observed in small auxin-upregulated *RNA 36* (*SAUR36*) and a gene encoding a purported auxin efflux carrier.

AA-treated plants showed induction of *PKS3L*, which encodes a precursor of the immune signaling peptide, phyto-sulfokine, a recently classified damage-associated molecular pattern (DAMP) (Zhang et al. 2018).

Unique transcriptional responses for ANE-treated roots at 24 h include those involved in auxin signaling, cytokinin biosynthesis, specialized plant metabolism, cell proliferation, and induced resistance. This included robust induction of *SAR8.2*, encoding a systemic acquired resistance protein, and *CKX2*, encoding cytokinin oxidase 2. Significant induction was also observed for *IAA2*, an auxin-regulated transcription factor. ANE-treated plants also showed upregulation of *TCMP-1*, a tomato metallopeptidase inhibitor. Modulation was also seen in two 2-oxoglutarate and Fe(II)-dependent oxygenase superfamily members.

These data collectively show AA and ANE locally and systemically alter the transcriptional profile of tomato through modulation of many defense-related genes.

### Phytohormone quantification.

AA and ANE modulate expression of genes associated with JA, SA, and ethylene phytohormone signaling and biosynthesis. Therefore, levels of selected phytohormones and phytohormone precursors were quantified via liquid chromatography-tandem mass spectrometry (LC-MS/MS) (Fig. 6). The JA precursor oxophytodienoic acid (OPDA) accumulated in the leaves of plants root-treated with AA and ANE at 48 h, while accumulation of JA and its isoleucine conjugate (N-jasmonyl-L-isoleucine [JA-Ile]) occurred in the roots of AA-treated roots at 24 h. This coincides with induction of JA signaling components *JA2*, *JA2L*, *SIJAZ7*, and *SIJAZ11* in the roots of AA-treated plants at 24 h (Fig. 5). SA accumulated in roots of AA-treated plants at both sample timepoints, consistent with our observation of transcriptional upregulation of *NPR1* and *PR1* (Fig. 5). Elevated levels of SA also were seen in leaves of seedlings root-treated with AA and ANE at 48 h. Abscisic acid (ABA) increased in leaf tissue 24 and 48 h after root treatment with AA or ANE. Indole-3-acetic acid (IAA) and its aspartate conjugate (N-(3-indolylacetyl)-DL-aspartic acid [IAA-Asp]) and zeatin riboside isomers were reduced at 24 h in the roots of both AA-treated and ANE-treated plants. These changes in accumulation of IAA and its conjugate are consistent with the unique differential gene expression in *SAUR36* and a gene encoding a purported auxin efflux carrier in AA-treated roots at 24 h. Likewise altered levels of IAA and IAA-Asp also coincide with the unique induction of *IAA2*, an auxin-regulated transcription factor, in the roots of ANE-treated plants at 24 h (Supplementary Table S3). The leaves of plants whose roots were treated with AA and ANE also had reduced levels of zeatin ribosides at 24 and 48 h. Taken together, these data demonstrate that AA and ANE both alter the accumulation of multiple phytohormones, including those that modulate defense networks in tomato.

### Local and systemic induced resistance.

Given the overlapping transcriptional profiles and clear changes in phytohormone accumulation induced by AA and ANE root treatment, we utilized disease assays to establish the systemic nature of AA-induced resistance and to investigate the local and systemic nature of ANE-induced resistance. Roots pre-treated with AA, ANE, or H<sub>2</sub>O were

inoculated with zoospores of the oomycete *P. capsici* and seedlings were then evaluated for collapse due to root and crown rot. Postinoculation, 85% of plants treated with H<sub>2</sub>O collapsed at the crown while less than 20% of the ANE-treated plants collapsed. Treatment of roots with 0.4% ANE protected seedlings against *Phytophthora* root and crown rot compared with control seedlings treated with H<sub>2</sub>O and inoculated (Fig. 7A and C). Level of protection with ANE is similar to that observed with AA-induced resistance in tomato and pepper to *P. capsici* infection, using this same assay format (Dye and Bostock 2021).

The leaves of plants with roots treated with AA, ANE, or H<sub>2</sub>O were challenged with the bacterial pathogen *Pseudomonas syringae* pv. *tomato*. Both AA and ANE root treatments induced systemic resistance to *Pseudomonas syringae* pv. *tomato*. The leaves of seedlings that had been root-treated with either AA or ANE showed significantly reduced bacterial colonization 72 h postinoculation (hpi) compared with control seedlings treated with H<sub>2</sub>O and inoculated (Fig. 7B), with leaf symptoms corresponding to treatment effects on colonization (Fig. 7E). H<sub>2</sub>O control plants showed an average bacterial titer of 7.06 log colony-forming units per square centimeter, with AA- and ANE-treated plants showing a 1.25- and 1.35-fold decrease in bacterial growth, respectively. The observed leaf symptoms 72 hpi were also consistent with differences in bacterial colonization. These experiments demonstrate that both AA and ANE induced local and systemic resistance to subsequent infection with an oomycete pathogen after root inoculation or a bacterial pathogen after leaf inoculation.

#### **Direct effect of ANE on plant growth and zoospore motility.**

A tradeoff often occurs between plant growth and defense, which is frequently observed in seedlings after treatment with high concentrations of MAMPs, resulting in seedling growth inhibition (Gómez-Gómez et al. 1999). Therefore, we investigated the effect of ANE on plant growth in a hydroponic system. Direct treatment of tomato roots with 0.4% ANE significantly reduced fresh weight biomass compared with water at 72 h post-treatment, consistent with an ANE-associated growth penalty (Supplementary Fig. S4A). The ANE growth penalty is observed locally in treated roots (Supplementary Fig. S4B) and distally in shoots (Supplementary Fig. S4C), consistent with the ability of ANE to systemically alter the transcriptional profile and induce resistance.

Typically, MAMPs are thought to primarily act to inhibit pathogen proliferation through direct perception and defense activation in the plant. However, ANE is a complex mixture with many potentially bioactive compounds. Because a potential direct effect of ANE on zoospores of *Phytophthora* spp. has not been reported, we investigated effect of ANE on zoospore integrity and encystment. In a concentration-dependent manner, zoospores of *P. capsici* encyst and lyse in the presence of ANE (Fig. 7D). Zoospores exposed to dilute ANE (0.1%) showed abnormal motility or premature encystment compared with water controls, while zoospores treated with 0.3% ANE showed premature encystment and lysis compared with water controls (Supplementary Table S4). These data demonstrate the ability of ANE to alter zoospore motility by inducing abnormal movement, encystment, and lysis. Therefore, components in ANE not only trigger defense in tomato but have the capacity to affect *P. capsici* zoospore behavior and viability following direct exposure.

## Discussion

AA and related eicosapolyenoic fatty acids are unusual elicitors of defense whose structural requirements for activity, absence from higher plants, and abundance in oomycete pathogens distinguish them as MAMPs (Robinson and Bostock 2015). *A. nodosum*, the brown alga from which ANE is derived, belongs to the same major lineage as oomycetes and contains AA as a predominant polyunsaturated fatty acid (van Ginneken et al. 2011). ANE is used commercially in crops as a biostimulant and may also help plants cope with biotic and abiotic stresses. Through comparative transcriptomic analysis, our study revealed that root treatment with AA or ANE locally and systemically induce similar yet distinct transcriptional profiles in tomato. Root treatment with AA or ANE alter the accumulation of defense-related phytohormones locally in treated roots and systemically in untreated leaves. This study also revealed the systemic nature of AA-induced resistance and the local and systemic nature of ANE-induced resistance in tomato against pathogens with different parasitic strategies.

Unlike canonical MAMPs that are perceived at the cell surface, AA is rapidly taken up by plant cells and metabolized, with significant incorporation into plant lipids (Preisig and Ku 1988; Ricker and Bostock 1992). Therefore, perception of AA and, by inference, the AA present in ANE is likely different or more complex than direct immune receptor-mediated MAMP recognition and signal transduction. AA can directly engage endogenous plant oxylipin metabolism via action of specific lipoxygenases (LOX) that use AA as a substrate (Andreou et al. 2009; Fournier et al. 1993; Göbel et al. 2001, 2002; Hwang and Hwang 2010; Véronési et al. 1996). This study demonstrates AA and ANE induce multiple overlapping local and systemic responses, with interesting parallels and key differences with canonical MAMPs.

AA and ANE locally and systemically alter transcriptional profiles of tomato with many shared and unique features. Varying levels of transcriptional overlap were seen across timepoints and tissues with up to 80% overlap in roots and up to 55% overlap in leaves between genes differentially expressed compared with water in AA- and ANE-treated plants (Fig. 3C). Similarly, the canonical MAMPs *elf18* and *flg22* induce distinct yet primarily overlapping transcriptional changes in *Arabidopsis thaliana* (Wan et al. 2019). More recent work in *Arabidopsis thaliana* compared the early transcriptional response of plants treated with diverse MAMPs and DAMPs, which elicited striking levels of transcriptional congruency at early timepoints (5 min to 3 h) (Bjornson et al. 2021). Like traditional MAMPs, AA and ANE also induce expression of genes associated with pathogen-triggered immunity, including several *WRKY* transcription factors and SA receptor *NPR1*, which also accumulates in response to *flg22* treatment in *Arabidopsis thaliana* (Bjornson et al. 2021; Chen et al. 2017). Despite being an “orphaned” MAMP that may have a different mode of perception, AA and, by inference, ANE still engage common transcriptional and hormone-mediated defenses.

Systemic resistance is often induced in plants treated with MAMPs and, thus, is considered a product of the immune response (Mishina and Zeier 2007). Root treatment with either AA or ANE protected plants locally from *P. capsici* and systemically from *Pseudomonas syringae*

*pv. tomato*. MAMP treatment is also commonly associated with plant growth inhibition due to a growth vs. defense tradeoff (Wang and Wang 2014). As plants prime defense, there can be downregulation of photosynthesis-related genes and a shift of photoassimilate from growth to defense, resulting in a growth penalty. Flg22 and elf18 treatment of *Arabidopsis thaliana* inhibits seedling growth (Gómez-Gómez et al. 1999). Likewise, AA at concentrations used to induce immunity can significantly reduce tomato seedling length and inhibit lateral root formation and cotyledon expansion (Dye and Bostock 2021). We found that tomato roots treated with 0.4% ANE in a hydroponic system display a significant reduction in root and shoot fresh weight (Supplementary Fig. S3). Our findings coincide with a systemic induced resistance phenotype and growth penalty associated with other well-characterized MAMPs.

Although there is striking overlap between AA and ANE and some MAMP-induced immune responses, there are also distinct differences in how AA and ANE potentially interact with immune signaling and defense. A previous gene expression study in tomato revealed AA root treatment strongly induces local and systemic expression of several key oxylipin pathway genes (Dye et al. 2020). Here, we show upregulation of the same subset of genes in response to ANE root treatment. Like AA, ANE also activates expression of  $\alpha$ -*DOX1* and *9-LOX*, both of which form fatty acid hydroperoxides representing a first step in the generation of plant oxylipins. Oxylipins can serve as signaling molecules to mediate plant responses to wounding, abiotic stress, and pathogen attack (Robinson and Bostock 2015). As with AA, ANE also induces expression of *9-DES*, which can produce novel antimicrobial divinyl ethers that may operate to help restrict *Phytophthora* infections (Weber et al. 1999). Orthologs of *9-LOX* and *9-DES* are present in pepper, potato, and tobacco, and the 9-LOXs in these species can use AA as a substrate (Andreou et al. 2009; Fournier et al. 1993; Göbel et al. 2001, 2002; Hwang and Hwang 2010; Véronési et al. 1996). Like AA, ANE induces expression of *AOS3*, which produces unstable allene oxides from 13-hydroperoxy fatty acids, the first committed step in JA biosynthesis. Previous work with an *aos* mutant in *Arabidopsis thaliana* established that an intact JA pathway was required for AA-induced resistance to *Botrytis cinerea* (Savchenko et al. 2010). The same study showed that AA treatment of *Arabidopsis* and tomato leaves increased JA and reduced SA levels in the plants, a treatment effect abolished in the case of the *Arabidopsis aos* mutant. These data highlight the critical role of oxylipin metabolism and, potentially, of oxidized products of AA to help trigger changes in defense hormone signaling.

In the present study, we found accumulation of OPDA, JA, and SA concurrently in tomato plants with an induced resistance phenotype whose roots were treated with AA and ANE. Similarly, Lal et al. (2018) found that *Arabidopsis thaliana* with phosphomimetic mutations in receptor-like kinase BIK1 displayed elevated levels of both SA and JA in noninfected and in *Pseudomonas syringae pv. tomato*-challenged plants. Our data suggest that modulation of JA and SA, classically antagonistic in induced resistance studies, is complex and nuanced in tomato in response to AA and ANE. These findings also suggest that AA and ANE can induce broad-spectrum resistance to pathogens that utilize different parasitic strategies.

While AA and ANE treatment have similar transcriptional outcomes in planta and share the ability to induce local and systemic resistance, ANE is a complex extract containing

eicosapolyenoic acids as well as additional potentially bioactive compounds. Early work with AA demonstrated that it has no direct effect on zoospore motility or viability of *P. infestans* and *P. capsici* (Ricker and Bostock 1994). In contrast, we found that direct exposure of *P. capsici* zoospores to ANE diminishes motility and viability in a concentration-dependent manner (Supplementary Fig. S4; Supplementary Table S4). However, our induced-resistance experimental format with *P. capsici* ensured that zoospores did not come into direct contact with inhibitory concentrations of ANE. Also, the relevance of our observation in field settings is unclear, since we would expect there to be substantial dilution of ANE during soil applications. Nonetheless, the potential to directly inhibit pathogen inoculum should be considered in experimental design in assessments of seaweed-derived and other biostimulants.

This study provides in-depth profiles of AA- and ANE-associated local and systemic transcriptional remodeling events, phytohormone changes, and induced resistance in tomato, with interesting parallels and differences with canonical MAMP action. Further investigation and functional analyses of oxylipin metabolism genes in relation to AA and ANE action is needed to help elucidate their potential role in MAMP signaling. Future research with eicosapolyenoic acid-containing biostimulants will lead to a more holistic understanding of diverse MAMP perception and response, with potential practical implications for crop disease management.

## Materials and Methods

### Disease and plant growth assays.

**Plant materials and hydroponic growth system.**—Seeds of tomato (*Solanum lycopersicum* cv. New Yorker) were surface-sterilized and were germinated for 10 days on germination paper. Seedlings were transferred to a hydroponic growth system in 0.5× aerated Hoagland's solution, contained in darkened plastic containers and maintained in a growth chamber with the following conditions: light intensity 150  $\mu\text{mol m}^{-2} \text{s}^{-1}$ , 16-h photoperiod, 24°C day, 22°C night, 65% relative humidity (Dye et al. 2020). The seedlings were incubated in the growth chamber for approximately 10 days, until emergence of two true fully expanded leaves. Seed was obtained from a commercial source (Totally Tomatoes, Randolph, WI, U.S.A.). New Yorker is a cultivar that we have used reliably in many studies under hydroponic conditions and it performs well with the treatments and in the disease assays used in this study.

**Root treatments.**—Fatty acid sodium salts (Na-AA and Na-LA) (Nu-Chek Prep, Elysian, MN, U.S.A.) were prepared and stored as previously described (Dye et al. 2020). A proprietary formulation of ANE (Acadian Seaplants, Ltd.) was diluted with deionized water ( $\text{diH}_2\text{O}$ ) to a 10% working concentration, which was used to prepare treatment dilutions. All chemicals were diluted to their treatment concentrations with sterile  $\text{diH}_2\text{O}$ . Hydroponically reared, 3-week-old tomato seedlings with two fully expanded true leaves were transferred to 1-liter darkened treatment containers. For *P. capsici* disease assays and ANE growth penalty assessments, roots were treated with an aerated 0.4% ANE solution or sterile  $\text{diH}_2\text{O}$  (control) for 72 h. For *Pseudomonas syringae* pv. *tomato* disease assays, roots were treated

with an aerated suspension of 10  $\mu\text{M}$  Na-AA, 0.4% ANE, or  $\text{diH}_2\text{O}$  for 72 h. Roots were soaked and rinsed as previously described (Dye and Bostock 2021). Treated seedlings were then returned to treatment containers with aerated 0.5 $\times$  Hoagland's solution for 72 h, followed by harvest for biomass measurements or inoculation with either *P. capsici* or *Pseudomonas syringae* pv. *tomato*. The concentrations of Na-AA (10  $\mu\text{M}$ ) and ANE (0.4%) used here induce optimal resistance in hydroponic New Yorker tomato seedlings against *P. capsici*, based on preliminary and previous studies. The concentration of ANE also falls within the range (0.2 to 0.4%) used in field applications.

***Phytophthora capsici* root inoculation and disease assessment.**—For root and crown disease assays, *P. capsici* isolate PWB-53 (Hensel) was used for inoculation. Tomato seedlings were individually inoculated with 5 ml of zoospore suspension ( $0.5 \times 10^4$  per milliliter) as described in (Dye et al. 2020). At 72 hpi, disease incidence was rated on the basis of seedling collapse at the crown. Pathogen cultures were maintained, inoculum was prepared, and seedling collapse was determined as previously described (Dileo et al. 2010; Dye et al. 2020; Dye and Bostock 2021).

***Pseudomonas syringae* pv. *tomato* inoculation and analysis of bacterial growth.**—For leaf disease assays, *Pseudomonas syringae* pv. *tomato* DC3000 was used for inoculation. *Pseudomonas syringae* pv. *tomato* from glycerol stock maintained at  $-80^\circ\text{C}$  was grown on nutrient yeast glycerol agar (NYGA) media amended with rifampicin at 100  $\mu\text{g}/\text{ml}$  for 2 days at  $28^\circ\text{C}$ . *Pseudomonas syringae* pv. *tomato* was restreaked on rifampicin-amended NYGA media and was grown for 24 h at  $28^\circ\text{C}$ . The bacteria were harvested and resuspended in 5 mM  $\text{MgCl}_2$ . Leaves were sprayed with a bacterial suspension of optical density at 500 nm = 0.3 with 0.01% Silwett, using a Preval spray system (Nokoma Products, Bridgefield, IL, U.S.A.). Plants were sprayed until runoff with abaxial and adaxial leaf surfaces covered. Cut Parafilm was used as a protective barrier around the base of plants to prevent contamination of the hydroponic system. Plants were covered with clear plastic bags for 48 hpi. Bacterial colonization was quantified by growth curve analysis 4 days postinoculation, as described by Liu et al. (2009).

#### **ANE growth penalty assay.**

After treatment and Hoagland's solution interval, tomato seedlings were harvested and roots were excised from shoots. Root and shoot tissue samples were individually weighed and fresh weights were recorded. Roots represent all below-surface plant tissue beneath the hypocotyl, and shoots represent all aerial tissue including leaves.

#### **3' Batch tag sequencing assay.**

**Root treatment, tissue harvest, and RNA extraction.**—For tissue samples for 3' batch tag sequencing, roots were treated with an aerated solution of 10  $\mu\text{M}$  AA, 10  $\mu\text{M}$  LA, 0.4% ANE, or  $\text{diH}_2\text{O}$ . Harvested tissue was then subjected to total RNA extraction, using Qiagen's RNeasy plant mini kit with off-column DNase digestion, using Qiagen's RNase-Free DNase set (Qiagen, Germantown, MD, U.S.A.). Each sample was the pool of roots or leaves of two seedlings with three replications per tissue, treatment, and timepoint. All samples were then submitted to the University of California-Davis Genome Center DNA

Technology Core for quality control via bioanalyzer analysis, RNA-seq library generation, and sequencing. Gene expression profiling was carried out using a 3'-tag-RNA-seq protocol. Barcoded sequencing libraries were prepared using the QuantSeq FWD kit (Lexogen, Vienna) for multiplexed sequencing, according to the recommendations of the manufacturer, using both the UDI-adaptor and UMI second-strand synthesis modules (Lexogen). The fragment size distribution of the libraries was verified via micro-capillary gel electrophoresis on a LabChip GX system (PerkinElmer, Waltham, MA, U.S.A.). The libraries were quantified by fluorometry on a Qubit fluorometer (LifeTechnologies, Carlsbad, CA, U.S.A.) and were pooled in equimolar ratios. The library pool was Exonuclease VII-treated (NEB, Ipswich, MA, U.S.A.), SPRI bead-purified with KapaPure beads (Kapa Biosystems, Roche, Basel, Switzerland), and were quantified via quantitative PCR with a Kapa Library Quant kit (Kapa Biosystems) on a QuantStudio 5 reverse transcription-PCR system (Applied Biosystems, Foster City, CA, U.S.A.). Up to 48 libraries were sequenced, per lane, on a HiSeq 4000 sequencer (Illumina, San Diego, CA, U.S.A.) with single-end 100-bp reads.

**RNA-seq data processing and analysis.**—The raw reads were imported into the Galaxy platform for comprehensive data analysis including quality control, alignment, and differential expression analysis (Goecks et al. 2010). The raw data was processed using the quality control tool FastQC/MultiQC (v1.7) to assess the quality of the raw sequence data (Ewels et al. 2016). Read alignment was conducted using RNA STAR aligner (v2.6.0b-1) and post-alignment quality control employed FastQC/MultiQC (v1.7) (Ewels et al. 2016). Quantification of reads per gene was carried out using featureCounts (v1.6.3) (Liao et al. 2013). Read counts were normalized and differential gene expression analysis was conducted using DESeq2 (v2.11.40.6) (Love et al. 2014). Differential genes were visualized using the Heatmap2 (v1.0) program, followed by functional enrichment of differential genes by the program GoSeq (1.34.0) (Young et al. 2010). All aforementioned bioinformatics programs were accessed through the Galaxy toolshed (Blankenberg et al. 2014). Differential gene expression was also visualized as volcano plots, developed using ggplot2 (v3.3.5) via a custom script (Supplementary File S1).

### Phytohormone quantification.

For phytohormone quantification, roots were treated with an aerated suspension of 10  $\mu$ M Na-AA (in deionized water), 0.4% ANE (in deionized water), or deionized water. Following 24 and 48 h of root exposure to their respective treatments, plants were harvested, root and leaf tissue was dissected from shoots, and the collected tissue was flash-frozen in liquid nitrogen. Root and leaf tissue samples were submitted to the Donald Danforth Plant Science Center Proteomics and Mass Spectrometry Facility for acidic plant hormone extraction and quantification. Each sample was the pool of roots and leaves of three seedlings with three samples per tissue, treatment, and timepoint. The experiment was performed once.

Analytical reference standards were used for the following analytes: IAA (Sigma-Aldrich St. Louis), IAA-Asp (Sigma-Aldrich), (+/-)-JA (Tokyo Chemical Industry Company, Tokyo), SA (Acros Organics, Geel, Belgium), (+/-)-ABA (Sigma-Aldrich), JA-Ile (Toronto Research Chemicals, Toronto, Canada), OPDA (Cayman Chemical, Kalamazoo, MI, U.S.A.), *cis*-zeatin (*cZ*) (Santa Cruz Biotechnology, Santa Cruz, CA, U.S.A.), *trans*-zeatin (*Z*) (Caisson

Labs, Smithfield, UT, U.S.A.), DL-dihydrozeatin (DHZ) (Research Products International, Mount Prospect, IL, U.S.A.), and Z riboside (ZR) (Gold Biotechnology, St. Louis). Internal standards were d<sub>5</sub>-JA (Tokyo Chemical Industry Company), d<sub>5</sub>-IAA (CDN Isotopes, Pointe-Claire, Canada), d<sub>5</sub>-dinor-OPDA (Cayman Chemical), d<sub>6</sub>-SA (CDN Isotopes), d<sub>6</sub>-ABA (ICON Isotopes, Dexter, MI, U.S.A.), d<sub>5</sub>-Z (OIChemIm, Olomouc, Czech Republic), d<sub>5</sub>-ZR (OIChemIm), <sup>13</sup>C<sub>6</sub> <sup>15</sup>N JA-Ile (New England Peptide, Gardner, MA, U.S.A.), and <sup>13</sup>C<sub>4</sub> <sup>15</sup>N IAA-Asp (New England Peptide). LC-MS grade methanol (MeOH) and acetonitrile (ACN) were sourced from J.T. Baker (Avantor Performance Materials, Radnor, PA, U.S.A.) and LC-MS grade water was purchased from Honeywell Research Chemicals (Mexico City). Standard and internal standard stock solutions were prepared in 50% methanol and were stored at -80°C. Calibration standard solutions were prepared fresh in 30% methanol.

**Phytohormone extraction.**—Phytohormones cZ, Z, DHZ, ZR, SA, ABA, IAA, IAA-Asp, JA, JA-Ile, and OPDA were extracted at a tissue concentration of 100 mg/ml in ice cold 1:1 MeOH/ACN. Around 100 mg of tissue sample were weighed and 10 µl of mixed stable isotope-labeled standards (1.0 µM for d<sub>5</sub>-Z and d<sub>5</sub>-ZR, 2.5 µM for d<sub>4</sub>-SA, d<sub>6</sub>-ABA, d<sub>5</sub>-JA, d<sub>5</sub>-IAA, <sup>13</sup>C<sub>6</sub> <sup>15</sup>N-IAA-Asp and d<sub>5</sub>-dinor-OPDA, and 25.0 µM for <sup>13</sup>C<sub>6</sub> <sup>15</sup>N-JA-Ile) were added to each sample prior to extraction. The samples were homogenized with a TissueLyzer-II (Qiagen) for 5 min at 15 Hz and were then centrifuged at 16,000 × g for 5 min at 4°C. The supernatants were transferred to new 2 ml tubes and the pellets were re-extracted with 600 µL 1:1 ice cold MeOH: ACN. These extracts were combined and were dried in a vacuum centrifuge. The samples were then reconstituted in 100 µl of 30% methanol, were centrifuged to remove particulates, and were then passed through a 0.8-µm polyethersulfone spin filter (Sartorius, Stonehouse, U.K.), prior to dispensing into high-performance liquid chromatography vials for LC-MS/MS analysis.

**LC-MS/MS analysis.**—Phytohormones cZ, Z, DHZ, ZR, SA, ABA, IAA, IAA-Asp, JA, JA-Ile, and OPDA were quantified using a targeted multiple reaction monitoring (MRM) and isotope dilution-based LC-MS/MS method. A Shimadzu Prominence-XR UFLC system connected to a SCIEX hybrid triple quadrupole-linear ion trap mass spectrometer equipped with a Turbo V electrospray ionization source (SCIEX, Framingham, MA, U.S.A.) were used for the quantitative analysis. Reconstituted samples (10 µl) were loaded onto a 3.0 × 100 mm 1.8 µm ZORBAX Eclipse XDB-C<sub>18</sub> column (Agilent Technologies, Santa Clara, CA, U.S.A.) and the phytohormones were eluted within 22.0 min, in a binary gradient of 0.1% acetic acid in water (mobile phase A) and 0.1% acetic acid in 3:1 ACN/MeOH (mobile phase B). The initial condition of the gradient was 5% B from 0 to 2.0 min, ramped to 40% B at 10.0 min, further ramped to 50% B at 15.0 min, and, then, quickly raised to 95% B at 19.0 min and kept at 95% B until 22.0 min. The flow rate was set at 0.4 ml/min. Source parameters were set as follows: curtain gas 25 psi, source gas 140 psi, source gas 250 psi, collisionally activated dissociation gas set to 'medium', interface heater temperature 500°C, ion spray voltage set to +5,500 V for positive ion mode and -4,500 V for negative ion mode. Individual analyte and internal standard ions were monitored using previously optimized MRM settings programmed into a polarity switching method (cytokinins and auxins detected in positive ion mode, others detected in negative ion mode). Analyst 1.6.2 software (SCIEX) was used for data acquisition; MultiQuant 3.0.2 software (SCIEX) was

used for data analysis. The detected phytohormones were quantified based upon comparison of the analyte-to-internal standard integrated area ratios with a standard curve constructed using those same analytes, internal standards, and internal standard concentrations (2.5  $\mu\text{M}$   $^{13}\text{C}_6$   $^{15}\text{N}$ -JA-Ile, 0.10  $\mu\text{M}$   $d_5$ -IZ and  $d_5$ -IZR, others 0.25  $\mu\text{M}$ ). The mixed calibration solutions were prepared over the range from 1.0 fmol to 100 pmol loaded on the column. The actual calibration range for each analyte was determined according to the concentrations of the analyte in samples.

### ANE zoospore motility assay.

Aliquots of *P. capsici* zoospore suspension at  $10^6$  zoospores per milliliter were distributed to a polystyrene 96-well plate (Fisher Scientific, Hampton, NH, U.S.A.) and were exposed to ANE such that the final concentrations per well were 0.1, 0.2, 0.3, and 0.4% ANE. Sterile deionized water was used as a negative control. At 5, 10, and 15 min of exposure to their respective treatments, a hemocytometer was used to quantify vibrating and encysted zoospores per field of view. An overall motility status was also observed when fields of view with no motile zoospores remaining were reported. Using the standardized starting concentration, the overall motility status of the replicate, the sum of encysted and vibrating zoospores, and the number of lysed zoospores were calculated. Pathogen cultures were maintained and zoospore suspensions were prepared as previously described (Dye et al. 2020).

### Supplementary Material

Refer to Web version on PubMed Central for supplementary material.

### Funding:

Research supported in part by a Bill and Melinda Gates Foundation Millenium Scholars Program fellowship and Jastro-Shields awards to D. C. Lewis, United States Department of Agriculture National Institute of Food and Agriculture grant 2021-67034-35049 to D. M. Stevens, NIH grant R35GM136402 to G. L. Coaker, and an unrestricted gift from Acadian Seaplants LTD to R.M. Bostock. Sequencing was performed by the DNA Technologies and Expression Analysis Core at the UC Davis Genome Center, supported by NIH shared instrumentation grant 1S10OD010786-01. Phytohormone analyses were performed by the Donald Danforth Plant Science Center, St. Louis, based upon work supported by the National Science Foundation under grant number DBI-1427621 for acquisition of the QTRAP liquid chromatography-tandem mass spectrometry.

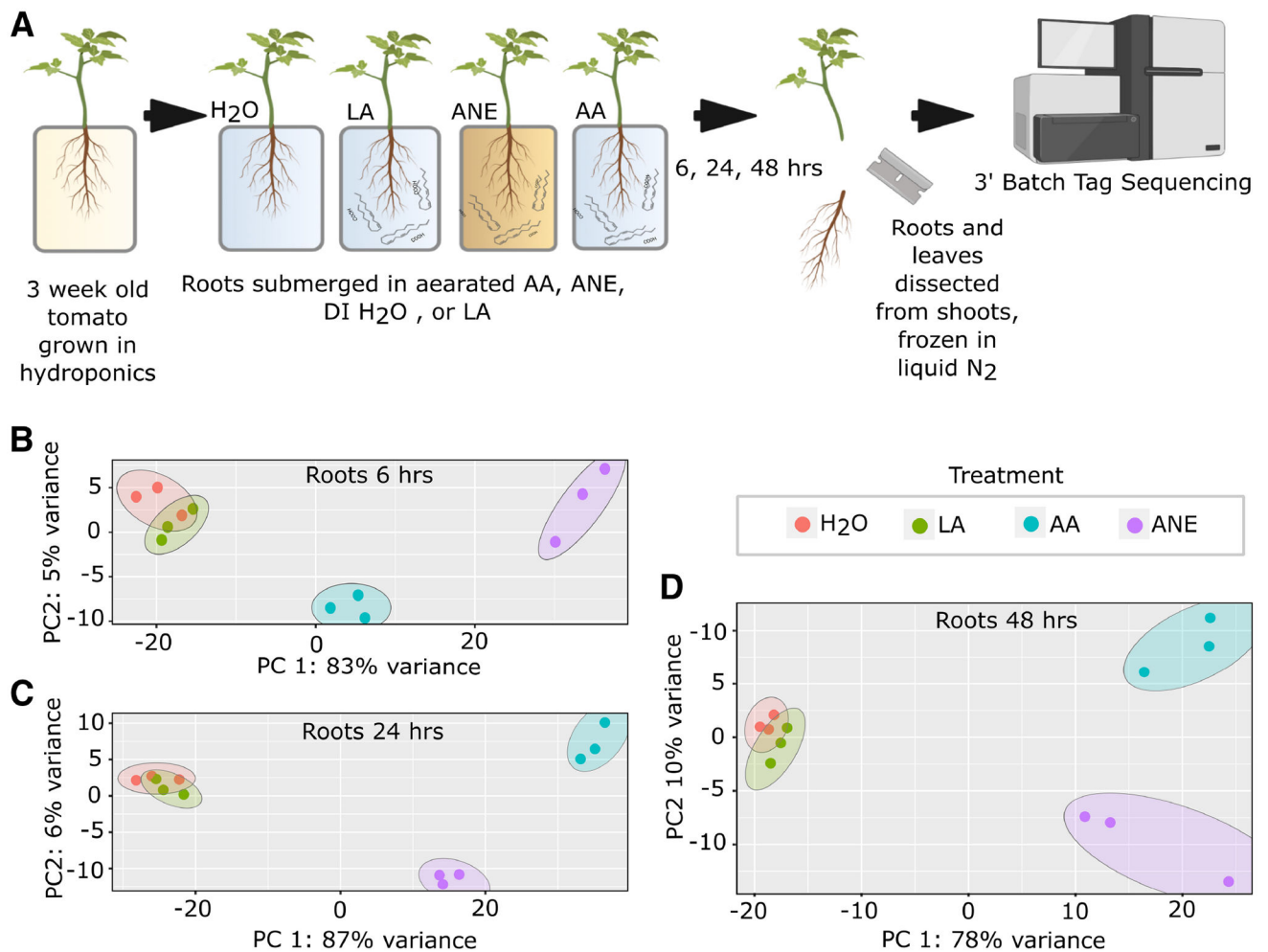
### Literature Cited

- Ali N, Ramkissoon A, Ramsubhag A, and Jayaraj J 2016. *Ascophyllum* extract application causes reduction of disease levels in field tomatoes grown in a tropical environment. *Crop Protect* 83:67–75.
- Andreou AZ, Hornung E, Kunze S, Rosahl S, and Feussner I 2009. On the substrate binding of linoleate 9-lipoxygenases. *Lipids* 44:207–215. [PubMed: 19037675]
- Araceli A-C, Elda C-M, Edmundo L-G, and Ernesto G-P 2007. Capsidiol production in pepper fruits (*Capsicum annuum* L.) induced by arachidonic acid is dependent of an oxidative burst. *Physiol. Mol. Plant Pathol* 70:69–76.
- Bjornson M, Pimprikar P, Nürnberger T, and Zipfel C 2021. The transcriptional landscape of *Arabidopsis thaliana* pattern-triggered immunity. *Nat. Plants* 7:579–586. [PubMed: 33723429]
- Blankenberg D, Von Kuster G, Bouvier E, Baker D, Afgan E, Stoler N, Taylor J, Nekrutenko A, and Galaxy T 2014. Dissemination of scientific software with Galaxy ToolShed. *Genome Biol* 15:403. [PubMed: 25001293]

- Bostock RM, Ku JA, and Laine RA 1981. Eicosapentaenoic and arachidonic acids from *Phytophthora infestans* elicit fungitoxic sesquiterpenes in the potato. *Science* 212:67–69. [PubMed: 17747631]
- Chen H, Chen J, Li M, Chang M, Xu K, Shang Z, Zhao Y, Palmer I, Zhang Y, McGill J, Alfano JR, Nishimura MT, Liu F, and Fu ZQ 2017. A bacterial type III effector targets the master regulator of salicylic acid signaling, NPR1, to subvert plant immunity. *Cell Host Microbe* 22:777–788.e7. [PubMed: 29174403]
- Chini A, Ben-Romdhane W, Hassairi A, and Aboul-Soud MAM 2017. Identification of TIFY/JAZ family genes in *Solanum lycopersicum* and their regulation in response to abiotic stresses. *PLoS One* 12: e0177381. [PubMed: 28570564]
- Choi D, Ward BL, and Bostock RM 1992. Differential induction and suppression of potato 3-hydroxy-3-methylglutaryl coenzyme A reductase genes in response to *Phytophthora infestans* and to its elicitor arachidonic acid. *Plant Cell* 4:1333–1344. [PubMed: 1283354]
- Cook J, Zhang J, Norrie J, Blal B, and Cheng Z 2018. Seaweed extract (Stella Maris®) activates innate immune responses in *Arabidopsis thaliana* and protects host against bacterial pathogens. *Mar. Drugs* 16: 221. [PubMed: 29958402]
- Creamer JR, and Bostock RM 1986. Characterization and biological activity of *Phytophthora infestans* phospholipids in the hypersensitive response of potato tuber. *Physiol. Mol. Plant Pathol* 28:215–225.
- Dave A, and Graham IA 2012. Oxylin signaling: A distinct role for the jasmonic acid precursor *cis*-(+)-12-oxo-phytodienoic acid (*cis*-OPDA). *Front. Plant Sci* 3:42. [PubMed: 22645585]
- Dileo MV, Pye MF, Roubtsova TV, Duniway JM, Macdonald JD, Rizzo DM, and Bostock RM 2010. Abscisic acid in salt stress predisposition to *Phytophthora* root and crown rot in tomato and chrysanthemum. *Phytopathology* 100:871–879. [PubMed: 20701484]
- Du M, Zhai Q, Deng L, Li S, Li H, Yan L, Huang Z, Wang B, Jiang H, Huang T, Li C-B, Wei J, Kang L, Li J, and Li C 2014. Closely related NAC transcription factors of tomato differentially regulate stomatal closure and reopening during pathogen attack. *Plant Cell* 26:3167–3184. [PubMed: 25005917]
- Dye SM, and Bostock RM 2021. Eicosapolyenoic fatty acids induce defense responses and resistance to *Phytophthora capsici* in tomato and pepper. *Physiol. Mol. Plant Pathol* 114:101642.
- Dye SM, Yang J, and Bostock RM 2020. Eicosapolyenoic fatty acids alter oxylin gene expression and fatty acid hydroperoxide profiles in tomato and pepper roots. *Physiol. Mol. Plant Pathol* 109:101444.
- Ewels P, Magnusson M, Lundin S, and Källner M 2016. MultiQC: Summarize analysis results for multiple tools and samples in a single report. *Bioinformatics* 32:3047–3048. [PubMed: 27312411]
- Fidantsef A, and Bostock R 1998. Characterization of potato tuber lipoxygenase cDNAs and lipoxygenase expression in potato tubers and leaves. *Physiol. Plant* 102:257–271.
- Fournier J, Pouéat M-L, Rickauer M, Rabinovitch-Chable H, Rigaud M, and Esquerré-Tugayé M-T 1993. Purification and characterization of elicitor-induced lipoxygenase in tobacco cells. *Plant J* 3:63–70.
- Gellerman JL, Anderson WH, Richardson DG, and Schlenk H 1975. Distribution of arachidonic and eicosapentaenoic acids in the lipids of mosses. *Biochim. Biophys. Acta* 388:277–290. [PubMed: 1138900]
- Göbel C, Feussner I, Hamberg M, and Rosahl S 2002. Oxylin profiling in pathogen-infected potato leaves. *Biochim. Biophys. Acta* 1584:55–64. [PubMed: 12213493]
- Göbel C, Feussner I, Schmidt A, Scheel D, Sanchez-Serrano J, Hamberg M, and Rosahl S 2001. Oxylin profiling reveals the preferential stimulation of the 9-lipoxygenase pathway in elicitor-treated potato cells. *J. Biol. Chem* 276:6267–6273. [PubMed: 11085991]
- Goecks J, Nekrutenko A, Taylor J, and Team G 2010. Galaxy: A comprehensive approach for supporting accessible, reproducible, and transparent computational research in the life sciences. *Genome Biol* 11:R86. [PubMed: 20738864]
- Gómez-Gómez L, Felix G, and Boller T 1999. A single locus determines sensitivity to bacterial flagellin in *Arabidopsis thaliana*. *Plant J* 18: 277–284. [PubMed: 10377993]

- Goñi O, Fort A, Quille P, McKeown PC, Spillane C, and O'Connell S 2016. Comparative transcriptome analysis of two *Ascophyllum nodosum* extract biostimulants: Same seaweed but different. *J. Agric. Food Chem* 64:2980–2989. [PubMed: 27010818]
- Hwang IS, and Hwang BK 2010. The pepper 9-lipoxygenase gene *CaLOXI* functions in defense and cell death responses to microbial pathogens. *Plant Physiol* 152:948–967. [PubMed: 19939946]
- Ishiga Y, Ishiga T, Uppalapati SR, and Mysore KS 2013. Jasmonate ZIM-domain (JAZ) protein regulates host and nonhost pathogen-induced cell death in tomato and *Nicotiana benthamiana*. *PLoS One* 8:e75728. [PubMed: 24086622]
- Jayaraj J, Wan A, Rahman M, and Punja ZK 2008. Seaweed extract reduces foliar fungal diseases on carrot. *Crop Protect* 27:1360–1366.
- Jogawat A, Yadav B, Chhaya, and Narayan OP 2021. Metal transporters in organelles and their roles in heavy metal transportation and sequestration mechanisms in plants. *Physiol. Plant* 173:259–275. [PubMed: 33586164]
- Klarzynski O, Descamps V, Plesse B, Yvin J-C, Kloareg B, and Fritig B 2003. Sulfated fucan oligosaccharides elicit defense responses in tobacco and local and systemic resistance against tobacco mosaic virus. *Mol. Plant-Microbe Interact* 16:115–122. [PubMed: 12575745]
- Knight VI, Wang H, Lincoln JE, Lulai EC, Gilchrist DG, and Bostock RM 2001. Hydroperoxides of fatty acids induce programmed cell death in tomato protoplasts. *Physiol. Mol. Plant Pathol* 59:277–286.
- Lal NK, Nagalakshmi U, Hurlburt NK, Flores R, Bak A, Sone P, Ma X, Song G, Walley J, Shan L, He P, Casteel C, Fisher AJ, and Dinesh-Kumar SP 2018. The receptor-like cytoplasmic kinase BIK1 localizes to the nucleus and regulates defense hormone expression during plant innate immunity. *Cell Host Microbe* 23:485–497.e5. [PubMed: 29649442]
- Liao Y, Smyth GK, and Shi W 2013. featureCounts: An efficient general purpose program for assigning sequence reads to genomic features. *Bioinformatics* 30:923–930. [PubMed: 24227677]
- Liu J, Elmore JM, Fuglsang AT, Palmgren MG, Staskawicz BJ, and Coaker G 2009. RIN4 functions with plasma membrane H<sup>+</sup>-ATPases to regulate stomatal apertures during pathogen attack. *PLoS Biol* 7:e1000139. [PubMed: 19564897]
- Lohman BK, Weber JN, and Bolnick DI 2016. Evaluation of TagSeq, a reliable low-cost alternative for RNA seq. *Mol. Ecol. Resour* 16: 1315–1321. [PubMed: 27037501]
- Lorenzo JM, Agregán R, Munekata PES, Franco D, Carballo J, ahin S, Lacomba R, and Barba FJ 2017. Proximate composition and nutritional value of three macroalgae: *Ascophyllum nodosum*, *Fucus vesiculosus* and *Bifurcaria bifurcata*. *Mar. Drugs* 15:360. [PubMed: 29140261]
- Love MI, Huber W, and Anders S 2014. Moderated estimation of fold change and dispersion for RNA-seq data with DESeq2. *Genome Biol* 15:550. [PubMed: 25516281]
- Meyer E, Aglyamova GV, and Matz MV 2011. Profiling gene expression responses of coral larvae (*Acropora millepora*) to elevated temperature and settlement inducers using a novel RNA-seq procedure. *Mol. Ecol* 20:3599–3616. [PubMed: 21801258]
- Mishina TE, and Zeier J 2007. Pathogen-associated molecular pattern recognition rather than development of tissue necrosis contributes to bacterial induction of systemic acquired resistance in *Arabidopsis*. *Plant J* 50:500–513. [PubMed: 17419843]
- Ngou BPM, Ding P, and Jones JDG 2022. Thirty years of resistance: Zig-zag through the plant immune system. *Plant Cell* 34:1447–1478. [PubMed: 35167697]
- Preisig CL, and Ku JA 1988. Metabolism by potato tuber of arachidonic acid, an elicitor of hypersensitive resistance. *Physiol. Mol. Plant Pathol* 32:77–88.
- Ricker KE, and Bostock RM 1992. Evidence for release of the elicitor arachidonic acid and its metabolites from sporangia of *Phytophthora infestans* during infection of potato. *Physiol. Mol. Plant Pathol* 41: 61–72.
- Ricker KE, and Bostock RM 1994. Eicosanoids in the *Phytophthora infestans*-potato interaction: Lipoxygenase metabolism of arachidonic acid and biological activities of selected lipoxygenase products. *Physiol. Mol. Plant Pathol* 44:65–80.
- Robinson SM, and Bostock RM 2015.  $\beta$ -glucans and eicosapolyenoic acids as MAMPs in plant-oomycete interactions: Past and present. *Front. Plant Sci* 5:797. [PubMed: 25628639]

- Sangha JS, Ravichandran S, Prithiviraj K, Critchley AT, and Prithiviraj B 2010. Sulfated macroalgal polysaccharides  $\lambda$ -carrageenan and  $\iota$ -carrageenan differentially alter *Arabidopsis thaliana* resistance to *Sclerotinia sclerotiorum*. *Physiol. Mol. Plant Pathol* 75:38–45.
- Savchenko T, Walley JW, Chehab EW, Xiao Y, Kaspi R, Pye MF, Mohamed ME, Lazarus CM, Bostock RM, and Dehesh K 2010. Arachidonic acid: An evolutionarily conserved signaling molecule modulates plant stress signaling networks. *Plant Cell* 22:3193–3205. [PubMed: 20935246]
- Shukla PS, Mantin EG, Adil M, Bajpai S, Critchley AT, and Prithiviraj B 2019. *Ascophyllum nodosum*-based biostimulants: Sustainable applications in agriculture for the stimulation of plant growth, stress tolerance, and disease management. *Front. Plant Sci* 10:655. [PubMed: 31191576]
- Stermer BA, and Bostock RM 1987. Involvement of 3-hydroxy-3-methylglutaryl coenzyme a reductase in the regulation of sesquiterpenoid phytoalexin synthesis in potato. *Plant Physiol* 84:404–408. [PubMed: 16665452]
- Subramanian S, Sangha JS, Gray BA, Singh RP, Hiltz D, Critchley AT, and Prithiviraj B 2011. Extracts of the marine brown macroalga, *Ascophyllum nodosum*, induce jasmonic acid dependent systemic resistance in *Arabidopsis thaliana* against *Pseudomonas syringae* pv. *tomato* DC3000 and *Sclerotinia sclerotiorum*. *Eur. J. Plant Pathol* 131: 237–248.
- Sun J-Q, Jiang H-L, and Li C-Y 2011. Systemin/jasmonate-mediated systemic defense signaling in tomato. *Mol. Plant* 4:607–615. [PubMed: 21357647]
- Sun X-C, Gao Y-F, Li H-R, Yang S-Z, and Liu Y-S 2015. Overexpression of SIWRKY39 leads to enhanced resistance to multiple stress factors in tomato. *J. Plant Biol* 58:52–60.
- Tsuda K, Sato M, Stoddard T, Glazebrook J, and Katagiri F 2009. Network properties of robust immunity in plants. *PLoS Genet* 5:e1000772. [PubMed: 20011122]
- van Ginneken VJ, Helsper JP, de Visser W, van Keulen H, and Brandenburg WA 2011. Polyunsaturated fatty acids in various macroalgal species from North Atlantic and tropical seas. *Lipids Health Dis* 10:104. [PubMed: 21696609]
- Vera J, Castro J, Gonzalez A, and Moenne A 2011. Seaweed polysaccharides and derived oligosaccharides stimulate defense responses and protection against pathogens in plants. *Mar. Drugs* 9:2514–2525. [PubMed: 22363237]
- Véronési C, Rickauer M, Fournier J, Pouénat ML, and Esquerré-Tugayé MT 1996. Lipoxygenase gene expression in the tobacco-*Phytophthora parasitica nicotianae* interaction. *Plant Physiol* 112: 997–1004. [PubMed: 8938408]
- Wan W-L, Zhang L, Pruitt R, Zaidem M, Brugman R, Ma X, Krol E, Perraki A, Kilian J, Grossmann G, Stahl M, Shan L, Zipfel C, van Kan JAL, Hedrich R, Weigel D, Gust AA, and Nürnberger T 2019. Comparing *Arabidopsis* receptor kinase and receptor protein-mediated immune signaling reveals BIK1-dependent differences. *New Phytol* 221:2080–2095. [PubMed: 30252144]
- Wang W, and Wang Z-Y 2014. At the intersection of plant growth and immunity. *Cell Host Microbe* 15:400–402. [PubMed: 24721568]
- Weber H, Chételat A, Caldelari D, and Farmer EE 1999. Divinyl ether fatty acid synthesis in late blight-diseased potato leaves. *Plant Cell* 11:485–494. [PubMed: 10072406]
- Young MD, Wakefield MJ, Smyth GK, and Oshlack A 2010. Gene ontology analysis for RNA-seq: Accounting for selection bias. *Genome Biol* 11:R14. [PubMed: 20132535]
- Zhang H, Hu Z, Lei C, Zheng C, Wang J, Shao S, Li X, Xia X, Cai X, Zhou J, Zhou Y, Yu J, Foyer CH, and Shi K 2018. A plant phytosulfokine peptide initiates auxin-dependent immunity through cytosolic Ca<sup>2+</sup> signaling in tomato. *Plant Cell* 30:652–667. [PubMed: 29511053]

**Fig. 1.**

**A**, Experimental procedure for RNA sequencing. Tomato roots treated with 10  $\mu$ M arachidonic acid (AA), 0.4% Acadian (ANE), H<sub>2</sub>O, or 10  $\mu$ M linoleic acid (LA). Following 6, 24, and 48 h of root exposure to their respective treatments, plants were harvested, root and leaf tissue was dissected from shoots, and the collected tissue was flash frozen in liquid nitrogen. Harvested tissue was then subjected to total RNA extraction and DNase treatment. All samples were submitted for quality control, RNA-seq library construction, and 3' batch tag sequencing. **B**, Principal component analysis (PCA) scatterplots of RNA sequencing data in roots after 6, **C**, 24, and **D**, 48 h of treatment with 10  $\mu$ M AA, 0.4% ANE, H<sub>2</sub>O, or 10  $\mu$ M LA. PCA was conducted using the normalized read counts for all samples. PCA plots show variance of three biological replicates performed per timepoint and treatment.

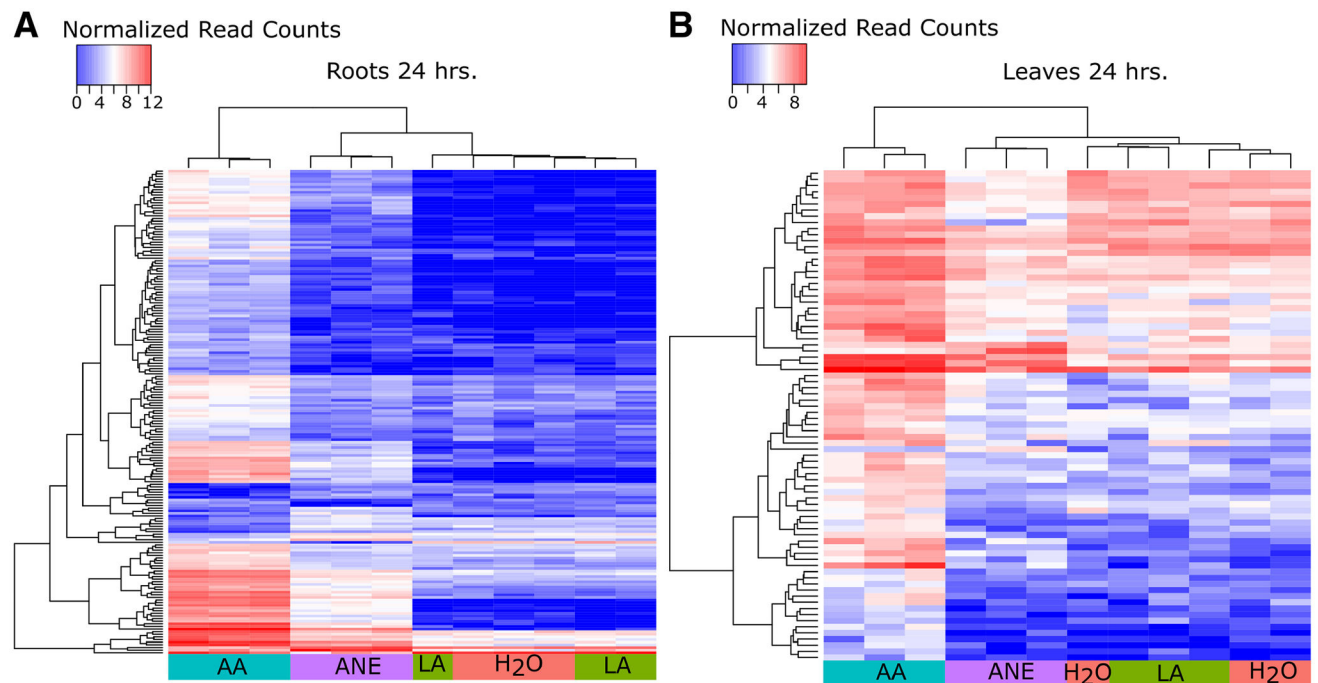


**Fig. 2.**

**A**, Normalized counts for the most differentially expressed genes by fold change for all treatment groups at 24 h in root and **B**, leaf tissue. Plant roots were treated 10  $\mu$ M arachidonic acid (AA), 0.4% Acadian (ANE), H<sub>2</sub>O, or 10  $\mu$ M linoleic acid (LA) for 24 h. Blue indicates significant gene suppression and red indicates significant gene induction for each treatment. Heatmap data is log<sub>2</sub>-transformed and hierarchically clustered. Differentially expressed genes require an adjusted *P* value <0.05 and an absolute fold change in gene expression >4 for roots and >2 for leaves.

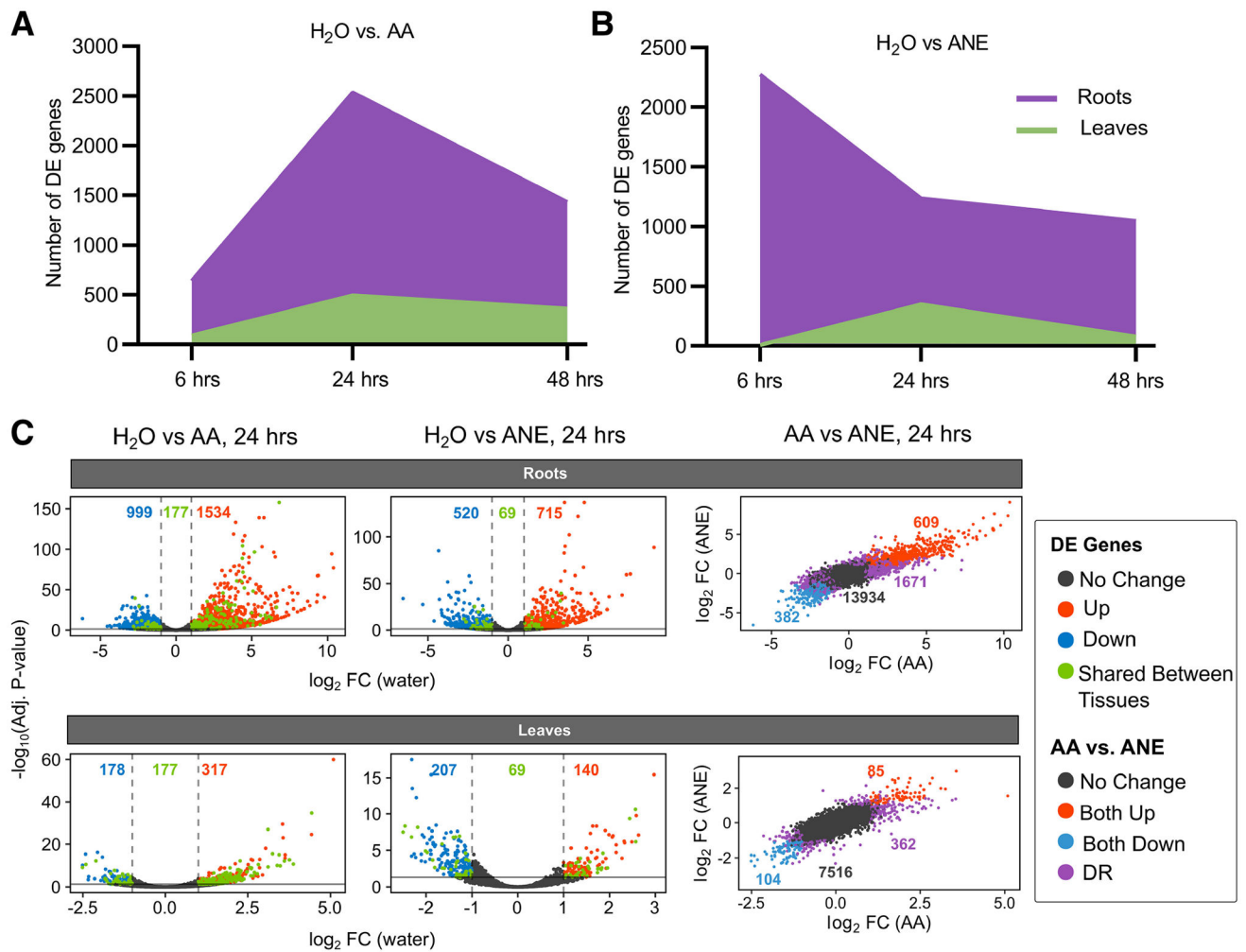


**Fig. 3.**

**A**, Total number of significant differentially expressed genes (DEGs) compared with H<sub>2</sub>O by tissue across timepoints for arachidonic acid (AA) and **B**, Acadian (ANE) root-treated tomato. Plant roots were treated with H<sub>2</sub>O, 10  $\mu$ M linoleic acid (LA), 10  $\mu$ M AA, or 0.4% ANE for 6, 24 or 48 h. **C**, Left: a scatter plot of DEGs with the number of significantly up-regulated (red) and downregulated (blue) genes plotted at 24 h from roots and leaves treated with AA or ANE compared with H<sub>2</sub>O. Those DEGs shared between tissues within a treatment are green. Solid and dashed lines represent cutoffs for significant DEGs (adjusted *P* value <0.05 and an absolute fold change in gene expression >2). Right: a scatter plot of gene expression in response to AA vs. ANE within the same tissue colored by differential response: both no change (gray), upregulated (red), and downregulated (blue) using the same significant cutoffs. Genes with different response (DR) between treatments are purple.

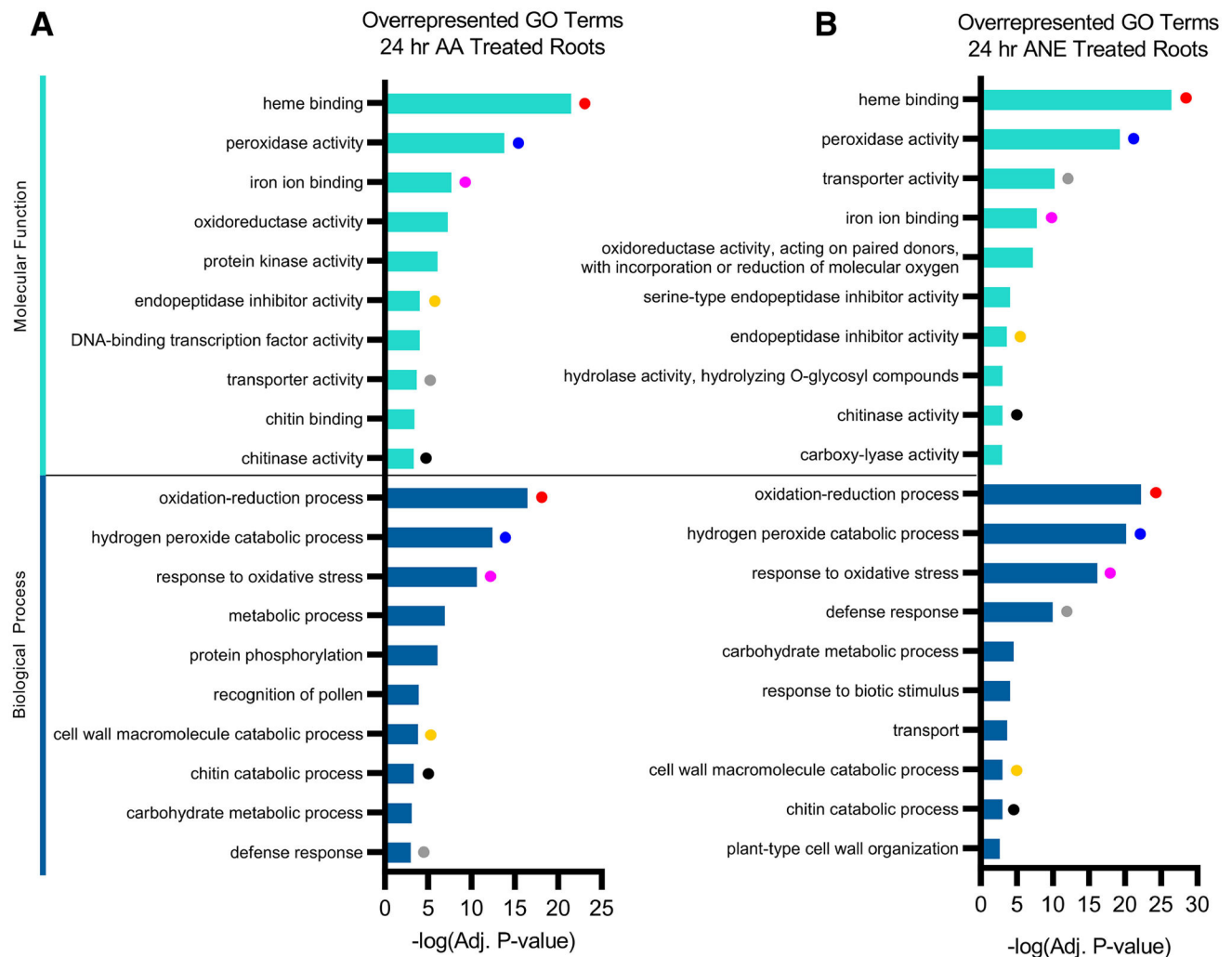


**Fig. 4.** Gene ontology (GO) functional analysis of differentially expressed genes in roots 24 h after treatment. GO enrichment was conducted using Goseq. The top 10 most significantly ( $P$  value  $<0.05$ ) enriched GO terms in molecular function and biological process GO categories are shown. Colored dots indicate shared molecular function and biological processes between **A**, arachidonic acid (AA) and **B**, Acadian (ANE) treatments. All adjusted  $P$  values are negative 10-base log-transformed.

Pathway	Gene ID	Annotation	Gene Name	AA 24 hr Roots		ANE 24 hr Roots	
				Log <sub>2</sub> FC	adj. p-value	Log <sub>2</sub> FC	adj. p-value
LOX Pathway	Solyc02g087070.3	alpha-DOX1	α-DOX1	6.656877	3.952504e-43	4.735599	2.393123e-21
	Solyc01g109140.3	divinyl ether synthase (9-divinyl ether synthase)	DES	6.451561	5.252232e-97	4.057925	6.092980e-32
	Solyc08g029000.3	Lipoxygenase (AHRD V3.3 *** Q43800_TOBAC)	9-LOX	5.670189	6.059722e-104	3.991129	3.722707e-45
	Solyc10g007960.1	Allene oxide synthase (AHRD V3.3 *** Q5NDE2_SOLTU) (Allene oxide synthase 3)	AOS3	1.685647	3.360501e-04	2.371630	5.336512e-04
WRKY TFs	Solyc05g015850.3	WRKY transcription factor 75	SIWRKY75	7.074404	2.312198e-50	5.419730	1.650934e-33
	Solyc08g067340.3	WRKY transcription factor 46	SIWRKY46	4.277548	3.244409e-13	2.881808	2.501558e-05
	Solyc03g116890.3	WRKY transcription factor 39	SIWRKY39	3.642748	8.280043e-32	1.874182	8.433876e-07
	Solyc09g015770.3	WRKY transcription factor 81	SIWRKY81	3.306811	1.054946e-35	1.735481	6.997109e-06
MAPKs	Solyc02g090970.1	MAP kinase kinase kinase 21	NA	5.000521	3.058998e-10	2.458481	6.761017e-03
	Solyc02g071740.3	MAP kinase kinase kinase 16	NA	2.606496	1.181915e-25	1.029662	1.057492e-03
Receptors	Solyc07g008620.1	EIX receptor 1	EIX1	3.669240	3.272107e-08	2.214993	8.598968e-03
	Solyc06g071810.1	Leucine-rich repeat receptor-like kinase (AHRD V3.3 *** K4C8Q3_SOLLG)	SOBIR1	1.886638	4.219792e-08	1.218518	4.244156e-03
JA Signaling	Solyc07g063410.3	JA2-like	JA2L	3.992618	4.410113e-13	2.044361	9.816992e-03
	Solyc12g013620.2	jasmonic acid 2	JA2	5.082760	5.312364e-12	3.668141	2.790927e-07
	Solyc08g036660.3	Jasmonate zim-domain protein (AHRD V3.3 *** G7IP70_MEDTR)	SIJAZ11	6.727738	7.883234e-15	2.877514	1.674547e-03
SA Signaling	Solyc11g011030.2	Pto-responsive gene 1	SIJAZ7	3.293363	2.058116e-07	2.035988	9.624008e-03
	Solyc07g044980.3	NIM1-like protein 2	NML2/ NPR1	1.168013	5.142510e-07	1.082963	8.851628e-07
Ethylene Signaling	Solyc09g066360.1	Ethylene Response Factor C.3	ERFC.3	8.251996	9.922638e-26	4.436850	2.455116e-09
	Solyc09g089610.3	ethylene receptor-like protein (ETR6)	ETR6	3.249116	4.072273e-03	2.494971	8.128305e-03
	Solyc06g053710.3	ethylene receptor homolog (ETR4)	ETR4	3.011504	2.959852e-21	2.267110	3.805192e-11
	Solyc09g075420.3	ethylene response factor E.1	ERF2	1.932686	1.137574e-02	2.708430	7.191094e-17
2 <sup>o</sup> Metabolism	Solyc01g101170.3	Viridiflorene synthase (AHRD V3.3 *** TPS31_SOLLG)	TPS31	9.293983	2.134563e-35	5.660419	6.637793e-18
	Solyc04g072280.3	Laccase (AHRD V3.3 *** A0A022Q9N6_ERYGU)	NA	6.948967	3.476060e-16	3.697150	4.491432e-06
	Solyc02g038740.3	3-hydroxy-3-methylglutaryl coenzyme A reductase (AHRD V3.3 *** K4B5W7_SOLLG)	HMG2	6.546776	2.241348e-91	3.571600	2.001060e-21
	Solyc08g007790.3	3-hydroxy-3-methylglutaryl coenzyme A synthase	HMG5	4.819941	6.790517e-91	2.350877	4.449196e-16
	Solyc02g078650.3	Polyphenol oxidase (AHRD V3.3 *** A0A118JXA6_CYNCS)	NA	3.928785	5.125454e-134	2.310150	1.558317e-41
	Solyc08g068730.1	Tyramine n-hydroxycinnamoyl transferase (AHRD V3.3 *** Q5D8C0_CAPAN)	THT1-3	3.412020	4.833930e-29	2.571582	7.327733e-07
	Solyc10g011920.2	Phenylalanine ammonia-lyase (AHRD V3.3 *** A0A124SBF6_CYNCS)	PAL	3.735867	5.023393e-13	2.152346	1.365268e-03
Solyc04g049350.3	chorismate synthase 1 precursor (chorismate synthase 1)	CS1	1.663705	2.269832e-17	1.021305	2.146662e-09	
PR	Solyc06g061215.1	Proteinase inhibitor II (AHRD V3.3 *- B3F0C1_TOBAC)	NA	10.271308	4.417542e-95	7.396038	2.945058e-60
	Solyc06g076170.3	Glucan endo-1,3-beta-glucosidase, putative (AHRD V3.3 *** B9T3M9_RICCO)	NA	7.747762	3.541570e-27	5.511062	5.238145e-19
	Solyc00g174330.3	Pathogenesis related protein PR-1/Pathogenesis-related leaf protein 4	PR1 (P6)	6.520672	5.184005e-16	5.402830	5.765970e-22
	Solyc02g082920.3	acidic extracellular 26 kD chitinase	CHI3	5.870717	2.842767e-19	4.985453	3.760754e-20
	Solyc05g050870.3	Peroxidase (AHRD V3.3 *** K4C1C0_SOLLG)	NA	4.745316	1.246767e-10	4.424698	3.852836e-13
Solyc01g087820.2	subtilisin-like protease 4B	sbt4B	1.571173	3.557181e-07	1.748230	4.607271e-12	

**Fig. 5.** Significantly upregulated genes shared by arachidonic acid (AA)- and Acadian (ANE)-treated roots, at 24 h. Log<sub>2</sub>-fold change and adjusted *P* values of all genes are shown.

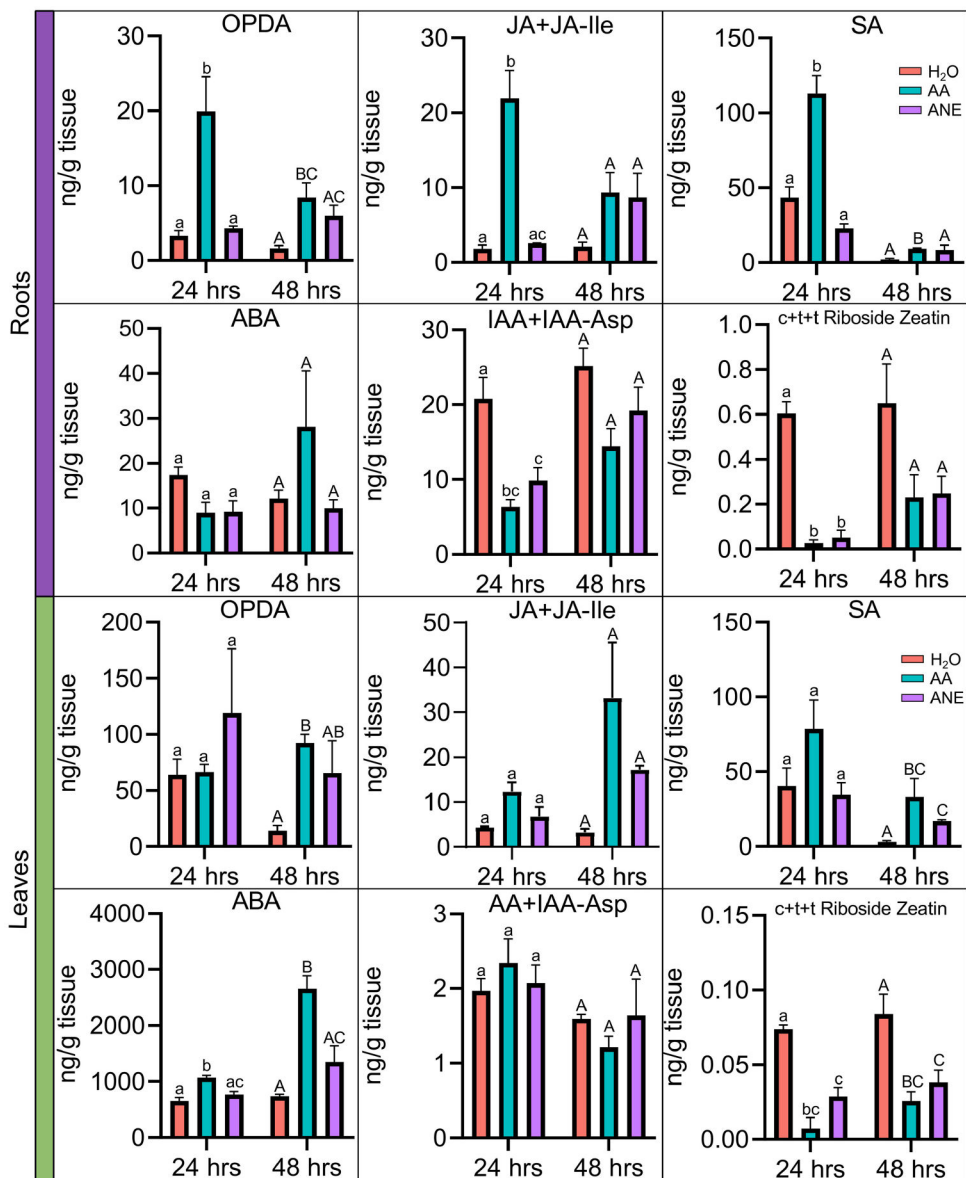


**Fig. 6.** Quantification of phytohormones oxophytodienoic acid (OPDA), jasmonic acid (JA) and JA-isoleucine (JA+JA-Ile), salicylic acid (SA), abscisic acid (ABA), indole acetic acid and IAA-aspartate (IAA+IAA-Asp), *cis/trans* zeatin and *trans* zeatin riboside in roots and leaves of tomato seedlings root-treated with H<sub>2</sub>O, 10  $\mu$ M arachidonic acid (AA), or 0.4% Acadian (ANE) for 24 and 48 h. Error bars represent standard error of three biological replicates. For bars with different letters, the difference of means is statistically significant by analysis of variance and Tukey's highly significant difference  $P < 0.05$ . Lower-case letters denote statistical significance for 24 h and upper-case letters denote statistical significance for 48 h. All statistical comparisons are within a single timepoint and tissue type.

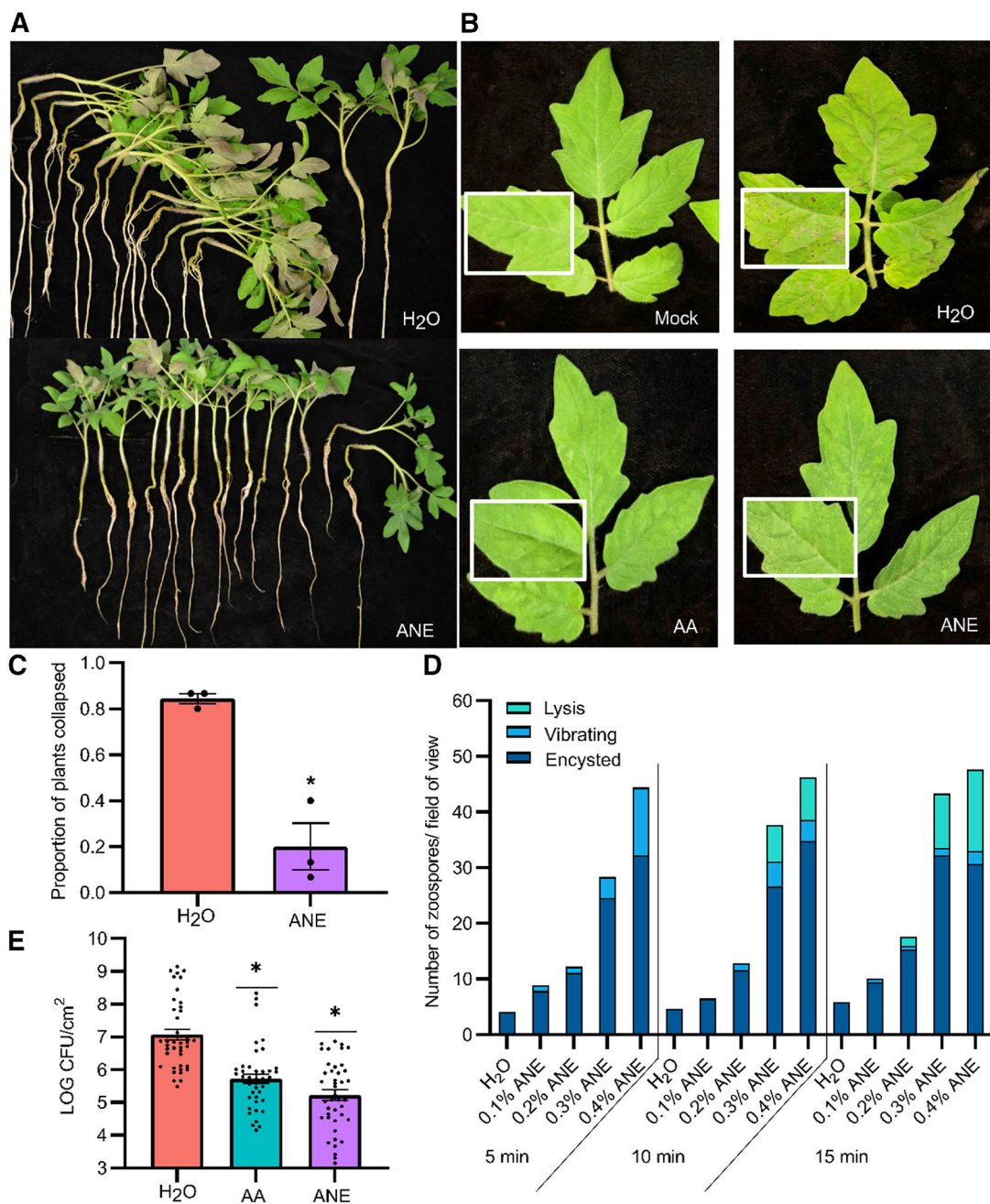


**Fig. 7.**

**A**, Hydroponically grown tomato seedlings treated with 0.4% Acadian (ANE) or H<sub>2</sub>O 48 h postinoculation with a *Phytophthora capsici* zoospore suspension and rated on the incidence of collapse at the crown. **B**, Representative leaf symptoms on hydroponically grown tomato root treated with 0.4% ANE, 10 μM arachidonic acid (AA), or H<sub>2</sub>O 72 h after spray inoculation with *Pseudomonas syringae* pv. *tomato* bacterial suspension in 10 mM MgCl<sub>2</sub> at optical density at 500 nm = 0.3. **C**, Proportion of plants treated with H<sub>2</sub>O or ANE that collapsed following inoculation with *P. capsici*. Data are the means and standard error (SE) for three independent trials at 0.4% ANE with 15 plants per treatment per trial. Asterisks

(\*) indicate significantly different by Wilcoxon rank sums test,  $X^2 = 3.97$ ,  $P < 0.046$ . **D**, Direct effect of 0.1, 0.2%, 0.3, and 0.4% ANE on zoospore motility at 5, 10, and 15 min of exposure. The number of lysed, vibrating, and encysted zoospores per field of view. Data are the means for three independent trials with  $n = 3$  per treatment concentration and timepoint per trial. **E**, Bacterial colonization as measured by LOG colony-forming units per square centimeter of leaf tissue 72 h postinoculation. Data are the means and SE for three independent trials with  $n = 14$  per trial. Asterisks (\*) indicate significantly different by Tukey's highly significant difference  $P < 0.0001$ .

Author Manuscript

Author Manuscript

Author Manuscript

Author Manuscript